NASA Technical Memorandum 74098

MEASUREMENTS AND ANALYSIS OF FAR-FIELD SCATTERING FROM A PROLATE SPHEROID

A. Bayliss and L. Maestrello

October 1977

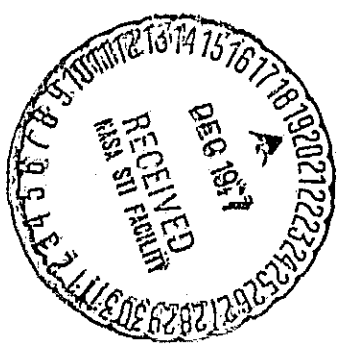

National Aeronautics and Space Administration

Langley Research Center
Hampton, Virginia 23665

MEASUREMENTS AND ANALYSIS OF FAR-FIELD SCATTERING FROM A PROLATE SPHEROID

A. Bayliss
Institute for Computer Applications in Science and Engineering
NASA Langley Research Center
Hampton, Virginia

L. Maestrello
NASA Langley Research Center
Hampton, Virginia

ABSTRACT

The far-field acoustic scattering by a prolate spheroid with axial point sources near the tip of the body was measured. Data were taken for ka between 10-160 where (a) is the semi-major axis of the spheroidal. Comparisons were made with numerical results obtained by an integral equation based on the simple source method, with appropriate coordinate stretching introduced to permit high frequency solutions with a minimal number of grid points. Theory and experiment agree within experimental error except for the highest frequencies in the shadow region, where very rapid changes in pressure make precise measurements difficult. The results show that for frequencies of aeroacoustic interest, the scattered field is very large and cannot be ignored.

I. INTRODUCTION

This paper is concerned with the scattering and diffraction of sound from a rigid prolate spheroid, with a source situated at a point along the major axis and near the tip of the body (see fig. 1).

The physical problem that motivated this work is to determine the scattering by an airplane fuselage, of the sound of a jet engine mounted on the axis and behind the body. This scattering is being neglected by the current schemes for flyover noise prediction, and it was the intention of the authors to test whether this neglect was justified. The airplane fuselage will be modeled by an elongated ellipsoid.

The far-field sound is a superposition of the incident field and the scattered field due to the presence of the body. A complete treatment of this problem requires the computation of the scattering with a variable flow over the body. This will permit the computation of the noise generated by an airplane in motion. Here we consider only the case of zero flow. The case of constant flow can be reduced to the case of zero flow by a Galilean transformation. A discussion of the effect of constant flow based on geometrical optics is given in reference 1.

Several techniques are available for the numerical computation of the scattered field. These are discussed in section 2. These methods were compared, and it was found that for the frequencies of interest, the integral equation method, using appropriate coordinate stretching, was best able to provide accurate solutions over the entire far field. This method and the stretching transformation which is crucial to its success is discussed in section 3.

In order to verify the accuracy of the numerical scheme an experiment was conducted. An experimental point source was placed near the tip of a spheroid with a shape that conforms to that of a typical airplane fuselage. The experiment is described in section 4 and the results are given in section 5.

The major conclusion of this paper is that the scattered field is a crucial component of the acoustic far field for frequencies of aeroacoustic interest. Prediction schemes which do not account for the scattering will not accurately describe the acoustic far field.

II. TECHNIQUES FOR NUMERICAL SOLUTION

The acoustic potential ϕ will be a solution of the wave equation, which reduces to the Helmholtz equation

$$\Delta\phi + k^2\phi = 0 \qquad (2.1)$$

in the frequency domain. Here k is the reciprocal wavelength. In order to work with nondimensional quantities we introduce the term ka where (a) is the semi-major axis. The solution to equation (2.1) becomes more difficult as ka increases because of the oscillatory behavior of the solutions. For aeroacoustic applications, however, (a) is required to be large, such that the solutions for $ka \geq 100$ will be required.

Three techniques are currently used to compute the scattered field:

1. Expansion in eigenfunctions
2. Integral equation methods
3. Asymptotic methods

The expansion in eigenfunctions, which is restricted to special bodies, is based on the fact that the Helmholtz equation is separable in the prolate spheroidal coordinate system. Thus, the solution can be written as an infinite series of the eigenfunctions of the separated operators (see reference 2). This series converges very slowly unless ka is small and thus this method is not suitable for the computation of aeroacoustic scattering and will not be considered further.

The integral equation method involves solving a Fredholm equation of the second kind over the surface of the scatterer. A general discussion of this method is given in reference 3 and a detailed discussion of its application to the present problem is given in section 3. The numerical solution of the equation for large values of ka can only be done efficiently if new coordinates are introduced on the body. If done properly, accurate solutions for values of ka of interest can be obtained. This method was used to generate the basic numerical results of this paper and for reasons to be described below, it is believed that this is the best of the three methods in obtaining solutions at aeroacoustic frequencies.

The third method, asymptotic expansion, includes both the conventional geometrical optics expansion and the theory of geometrical diffraction of J. Keller (see reference 4).

Geometrical optics involves obtaining the solution to the scattering problem by the method of ray tracing. Referring to figure 2, the total field at the point P is found by assuming a solution of the form

$$\phi = z(P)\frac{e^{iK|P - P^*|}}{4\pi|P - P^*|} + \phi_{inc}$$

where ϕ_{inc} is the incident wave. Here P* is the origin of the reflected wave going through P (see fig. 2) and z(P) is obtained through a principle of "conversion of energy" along ray tubes (see reference 2 for more details).

It is apparent from figure 2 that there is a region of space where no wave can penetrate. This is called the shadow region and the geometrical

optics approximation in this region $\phi = 0$. An improved approximation is obtained by the theory of geometrical diffraction as described in reference 4.

Referring to figure 3, rays incident on the curve of tangency C, excite surface rays (also called creeping waves) from which real waves are shed off tangent to the body. Analytical formulas have been developed for these diffracted waves (see for example reference 2, page 524).

Both these expansions are valid as $k \to \infty$. Geometrical optics requires ka large where (a) is the semi-major axis. Geometric diffraction, however, is based on the radius of curvature at the tip of the body and requires the wavelength to be small with respect to this length scale. Since any model of an airplane fuselage will be an elongated ellipsoid, this will have a relatively small radius of curvature and thus geometric diffraction will have a more restricted domain of validity than geometrical optics.

Results to be presented indicate that geometric diffraction is very inaccurate at frequencies of aeroacoustic interest. At the highest frequencies considered errors of the order of 5 decibels have been found. Geometrical optics also becomes inaccurate as the far-field point approaches the shadow region. Furthermore, it is found that the effect of the scattering is strongest in and near the shadow region. Thus, the integral equation method although more expensive than the asymptotic methods, is the only presently known method able to provide accurate numerical solutions in all regions of the far field, for the frequencies considered.

III. NUMERICAL SCHEME

The scattering problem described previously can be described mathematically as the solution to the following problem:

$$\text{a.}\quad \Delta_p + k^2\phi = -\delta(p - q) \tag{3.1}$$

$$\text{b.}\quad \phi_n = 0 \quad \text{on} \quad E$$

$$\text{c.}\quad \phi_r - ik\phi \to 0(r \to \infty)$$

where ϕ is the velocity potential. Here $k = \omega/c$ is the wave number, q is the source point, and E denotes the spheroid which models the airplane fuselage. We consider only axial sources so that the problem (3.1) is symmetric in the azimuthal direction (see fig. 1). The condition (3.1b) expresses the fact that the scattering is hard (zero normal velocity on the surface). The condition (3.1c) (the radiation condition) ensures that the problem (3.1) has a unique solution.

The problem (3.1) is set up for numerical solution by writing

$$\phi = \phi' + \phi^s$$

where ϕ^s is the singular part of the solution

$$\phi^s = \frac{e^{ik|p - q|}}{4\pi|p - q|}$$

and ϕ' is the scattered field and will be a solution to the problem

$$\text{a.}\quad \Delta\phi' + k^2\phi' = 0 \tag{3.2}$$

$$\text{b.}\quad \phi'_n = -\frac{\partial\phi^s}{\partial\phi_n} \quad \text{on} \quad E$$

$$\text{c.}\quad \phi'_r - ik\phi' \to 0 (r \to \infty)$$

The problem (3.2) is converted to an integral equation using the single layer potential method (see reference 3). One assumes a solution ϕ of the form

$$\phi'(p) = \iint_E \sigma(q)G(p,q)dA_q \tag{3.3}$$

where G is the free space Green's function

$$G(p,q) = \frac{e^{ik|p-q|}}{4\pi|p-q|}$$

and σ is to be determined. The physical interpretation of (3.3) is of a distribution of point sources with density σ such that the total field is the superposition of the field from each of the point sources.

On taking the normal derivative of (3.3) and letting the point p approach the surface E one obtains the surface Fredholm equation of the second kind for the unknown function σ (see reference 3)

$$\frac{\sigma(q)}{2} - \iint_{\partial E} dA_q \sigma(q')G_{n_q}(q,q') = -\phi_n(q) \tag{3.4}$$

where ϕ_n is the prescribed Neumann data (from (3.2b)).

If θ denotes the polar angle of the ellipsoid E (see fig. 1) then by the axial symmetry (3.4) can be converted into a one-dimensional equation

$$\frac{\sigma(\theta)}{2} - \int_{-\frac{\pi}{2}}^{\frac{\pi}{2}} d\theta' \sigma(\theta') H(\theta,\theta') = -\phi_n(\theta) \qquad (3.5)$$

where the kernel function $H(\theta,\theta')$ is the kernel in (3.4) integrated in the azimuthal direction and multiplied by the area factors.

There are two main difficulties associated with the equation (3.5). It is known that the equation will become singular if k is an eigenvalue of the interior Dirichlet problem. This problem of the interior resonances has been considered by various authors and the reader is referred to reference 3 for a comprehensive discussion of techniques for dealing with this problem.

It has been found that these singularities do not extend over a wide frequency range, and for the purpose of obtaining a power spectrum, this is not an important problem.

A much more critical problem is that of adequately resolving the solution at high frequencies. A measure of the oscillatory behavior of the solution is the nondimensional quantity ka where (a) is some length scale associated with the body. We will take (a) as the semi-major axis. The study of aeroacoustic scattering requires $ka \sim 100$ and at these frequencies many grid points are required. In order to obtain solutions at these frequencies, appropriate coordinates must be introduced.

Using an evenly spaced grid the equation (3.5) is converted to a linear system

$$\frac{\sigma(\theta_j)}{2} - h \sum_{\ell} \sigma(\theta_\ell) H(\theta_j, \theta_\ell) = -\phi_n(\theta_j) \qquad (3.6)$$

where h is the mesh spacing. The diagonal entry $H(\theta_j, \theta_j)$ is not a functional evaluation because of the singularity in the kernel function, but instead represents the integral of H across the singularity.

In order to obtain high frequency solutions with a minimal number of grid points new angular coordinates $\zeta(\theta)$ are introduced into the equation (3.5). Using an evenly spaced grid the equations (3.5) and (3.6) are entirely valid in the new coordinates except that the kernel function H will now be multiplied by $\frac{d\theta'}{d\zeta}$.

A 1-parameter family of new coordinates is introduced by the formula

$$\theta = \tan^{-1} \alpha \tan \zeta$$

where α is the free parameter. The parameter α is chosen so that the right hand side of (3.6) is smoothest in this coordinate system. This is described in more detail in reference 5 where numerical results show that high frequency solutions can be obtained with relatively coarse grid. For the ellipsoid considered here $\alpha = 5$ is optimal and the numerical solutions used here were generated with this parameter. On the basis of numerical tests described in reference 5, it is believed that for all frequencies considered, the solution generated by the integral equation is accurate to a relative error of 10 percent.

IV. EXPERIMENT

A prolate spheroidal body, figure 1, was constructed of hard fiberglass material with major axis length of 107.95 cm and with minor axis of 15.24 cm corresponding to an aspect ratio of 7.0833. The acoustic source consists of a 60 watt acoustic driver necked down to a small tubular opening. The driver is placed inside the body with the tube exiting at one tip and extending 1.9 cm outward. When driven by an oscillator at a discrete frequency, the output of this source consists of tones at the oscillator frequency and its harmonics. By appropriate filtering, the measured signal consists essentially of a discrete frequency.

This source possesses the well-known characteristic of radiating approximately uniformly in all directions in a stationary medium as long as the wavelength of the sound is considerably larger than the tube diameter (see reference 6). Since its physical operation consists of a time rate of mass fluctuation, it corresponds to an acoustic monopole. Three different tubes were used, ranging in size from 0.76 to 0.20 cm. The far-field intensity and directivity were experimentally established without the body in the range of frequencies between 1.4 to 16 KHz, over 180 degrees. The intensity field was constant to within 0.5 decibels about the arc except at the highest frequencies where correction was required.

The acoustic measurements were taken outdoors, and the model was placed 1.9 meters above the anechoic floor (see reference 7). Data were obtained on a circle centered at the source, with a radius of 10.9 meters corresponding to approximately 10 times the body length, a reasonable far-field distance.

Measurements were taken at 10 different angles from 0 degrees to 180 degrees where 0 degrees is the axis of the source. Pressure signals were measured with a 1.3 cm diameter condenser microphone and the data were passed through a bandpass filter, with the oscillating frequency set to an accuracy of ±1 Hz. The error of the electronic system, including readout, was estimated as within 0.5 decibels. The microphones were mounted level with the body on an especially designed arc support to minimize possible reflection from the mounting. The long distances between the microphones and source made precise positioning very difficult using conventional positioning methods. Because of this error, phases could not be accurately determined and are not reported on.

V. COMPARISON AND DISCUSSION OF RESULTS

Figures 4-6 are graphs of the decibel level change relative to the axial direction, as a function of the angle from the source. The graphs show the comparison between measured and computed results. The measured data were averaged over five readings taken at different times.

It is found that at low frequencies the scattered field is very small relative to the incident field except in the vicinity of the shadow region. This explains the flatness of graphs 4 and 5 near $\theta_0 = 0$. This effect is due to the slenderness of the body. Computations with wider spheroids at constant frequency show that scattering in directions near the axis increases as the body becomes spherical.

As the frequency varied from 1.4 KHz to 16.5 KHz, the dip in the shadow region increased by 5 db. This is the region of largest experimental

difficulty because of the sharpness of the dip, which increases with frequency and is sensitive to the angular position. Agreement even near this point is within experimental error except for the highest frequency where the dip is extremely sharp. The experimental data will, in general, give a smaller dip, because the microphones average a relatively large angular spread.

We note that as the wavelength decreases, the difference between minimum and maximum pressure increases and the pressure field itself becomes more oscillatory as a function of the far-field angle. For example, at 16.4 KHz the difference is of the order of 8 decibels, and this is roughly consistent with the measurements; for still higher frequencies the present measurement technique will have to be improved in order to resolve the rapidly oscillating acoustic pressure. At the lowest frequency of 1.41 KHz, the difference is only 2 decibels, and in the illuminated region the pressure is essentially flat. Thus, the scattered field in all regions of space becomes stronger as the frequency increases.

For the experimental body, the frequency of 16.4 KHz corresponds to a ka of 166 for a typical fuselage 70 meters long. This corresponds to a frequency of approximately .3 KHz which is near the peak of the jet noise spectra. Thus, the major conclusion is that scattering cannot be ignored for any aeroacoustic application and must be included in any prediction scheme.

The plot for 16.4 KHz includes comparison of results obtained by experiment, integral equation, and geometrical optics and diffraction. The

very large inaccuracy of the asymptotic method near the shadow region is evident. The integral equation has been applied for higher values of ka but will become expensive in storage and require spectral programming to obtain solutions out of core.

The 16.4 KHz solution could be generated in core because of a proper choice of the stretching parameter. A grid of 169 point was used on a Cyber 175 machine. The computation of the matrix (see (3.6)) required 105 sec. while the solution in the far-field can be computed in .9 sec. per point. The integral equation becomes more efficient the larger the number of field points required. From the figure for 16.4 KHz and from comparisons discussed in reference 5 it is apparent that geometrical optics provides accurate solutions except near the shadow region. Thus, in practice the integral equation method is required only near the shadow region, making it more costly per point. However, at present, no other method can provide accurate solutions in the vicinity of the shadow region.

REFERENCES

1. Padula, S. L.; and Liu, C. H.: Acoustic Scattering of Point Sources by a Moving Prolate Spheroid. AIAA Fourth Aeroacoustic Specialists Conference, Paper No. 77-1326, Atlanta, Georgia, October 1977.

2. Bowman, J. J., Sr.; and Uslenghi, P. L. E.: Electromagnetic and Acoustic Scattering by Simple Shapes. North Holland Publishing Company, Amsterdam, 1969.

3. Burton, A. J.: Numerical Solution of Scalar Diffraction Problems in Numerical Solution of Integral Equations. Delves and Walsh, Eds., Clarendon Press, Oxford, 1974.

4. Levy. B. R.; and Keller, J. B.: Diffraction by a Smooth Object. CPAM, 12, pp. 59-209, 1959.

5. Bayliss, A.: Numerical Computation of the Scattering of Scalar Waves at Intermediate Frequencies. ICASE Report No. 77-15, 1977.

6. Beranek, L. L.: Acoustics. McGraw-Hill Book Company, 1954.

7. Myles, M. M.; Ver, I. L.; and Henderson, H. R.: Effects of Outdoor Exposure on Sound Absorption Material. Journal of Sound and Vibration, June 1977.

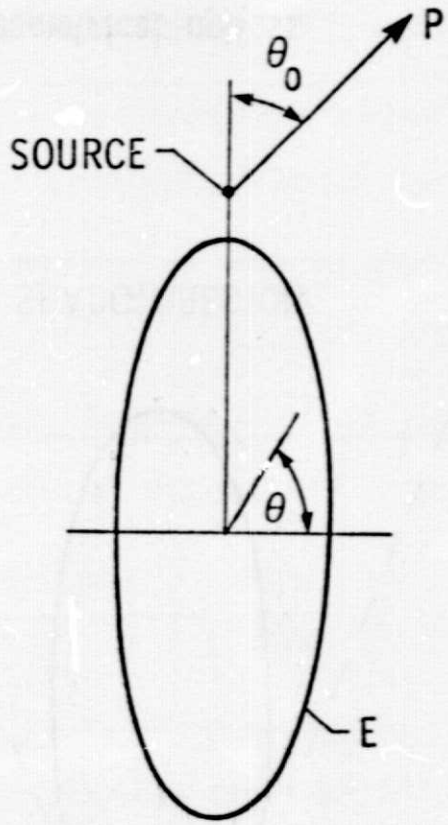

Figure 1. - Coordinate system of the ellipsoid.

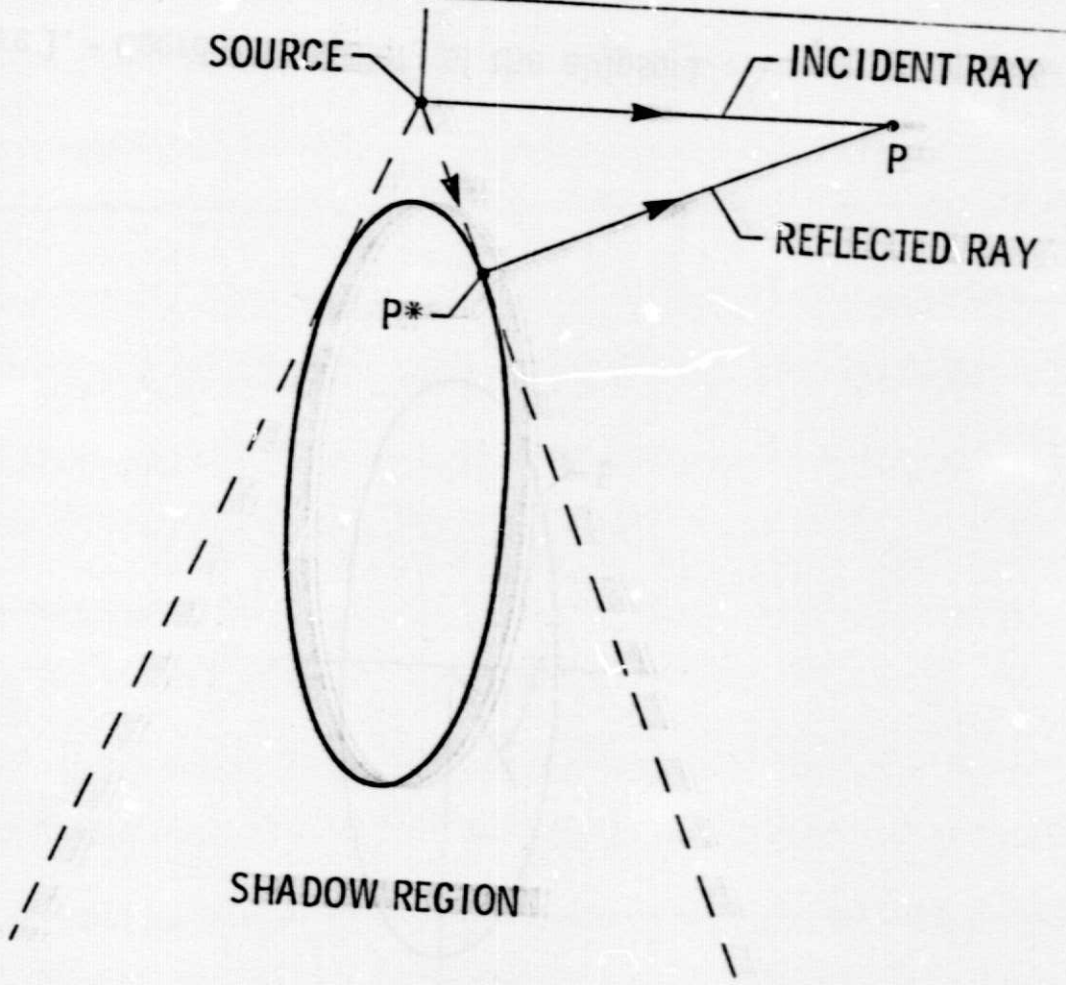

Figure 2. - Geometrical optics.

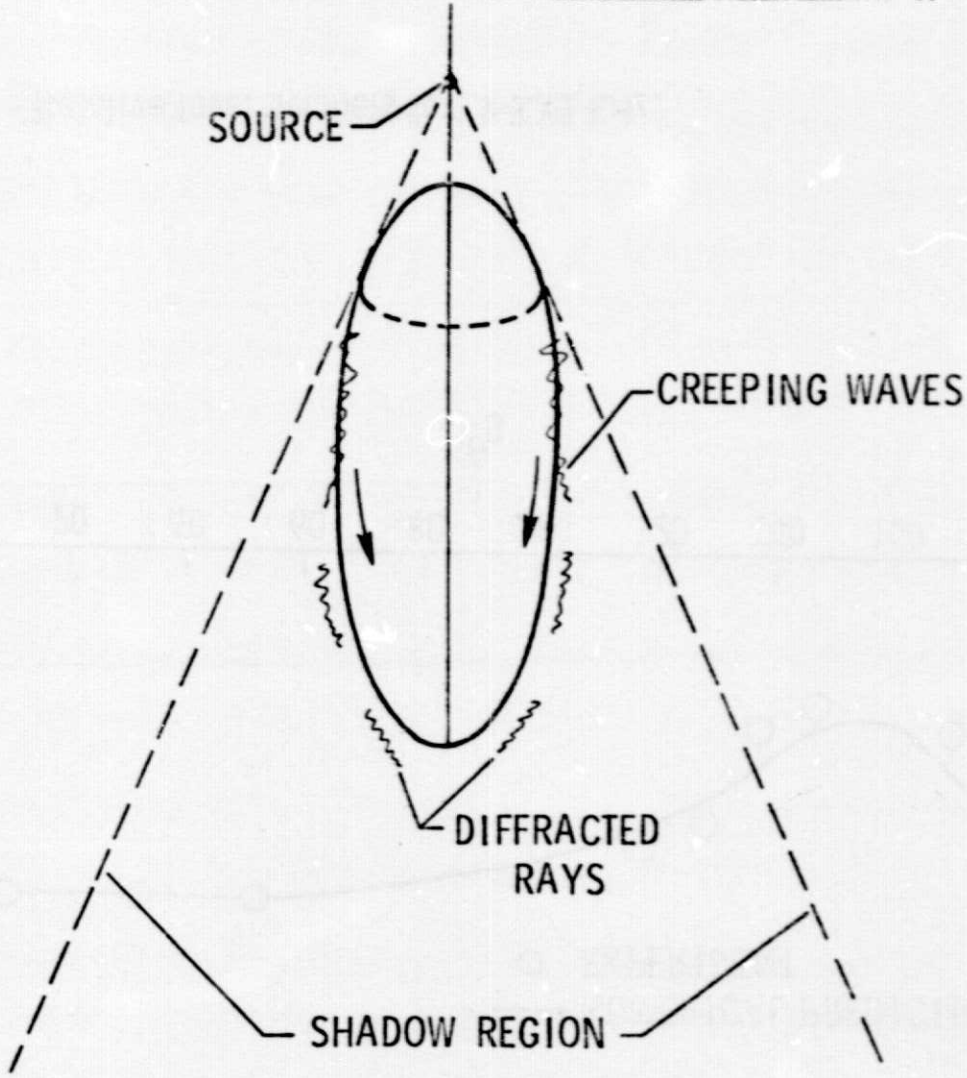

Figure 3. - Geometrical diffraction.

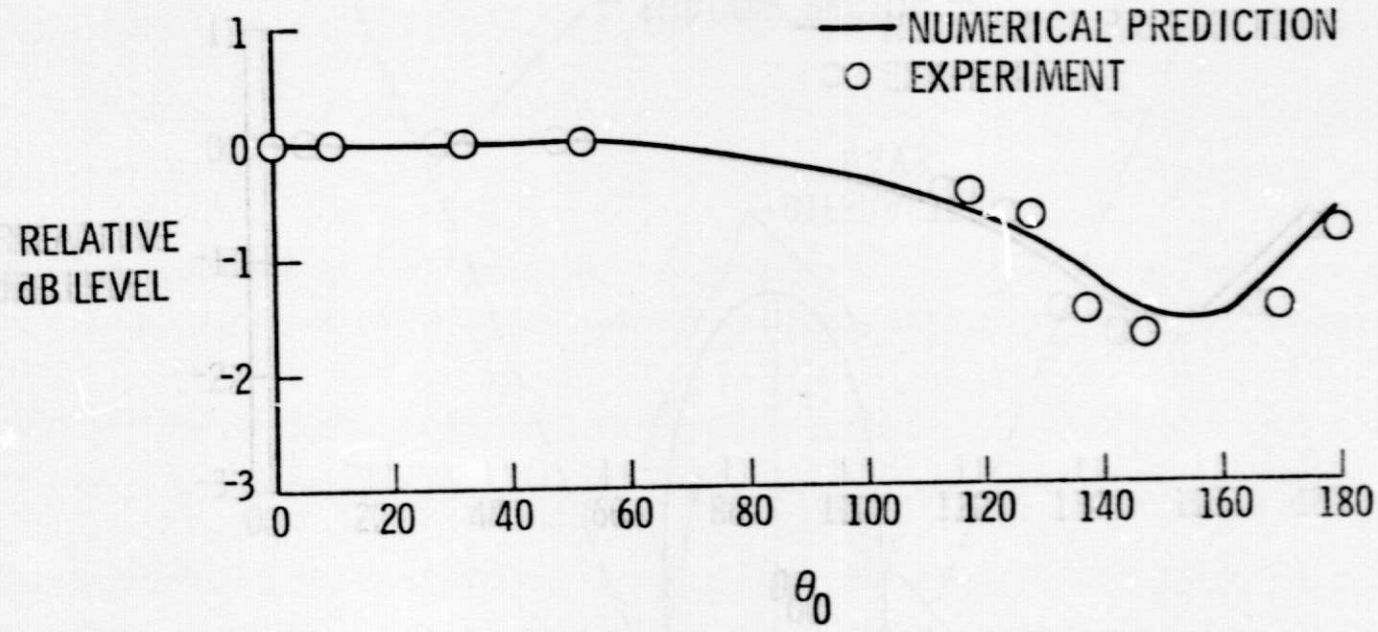

Figure 4. - Relative level decibels for f=1.41 kHz.

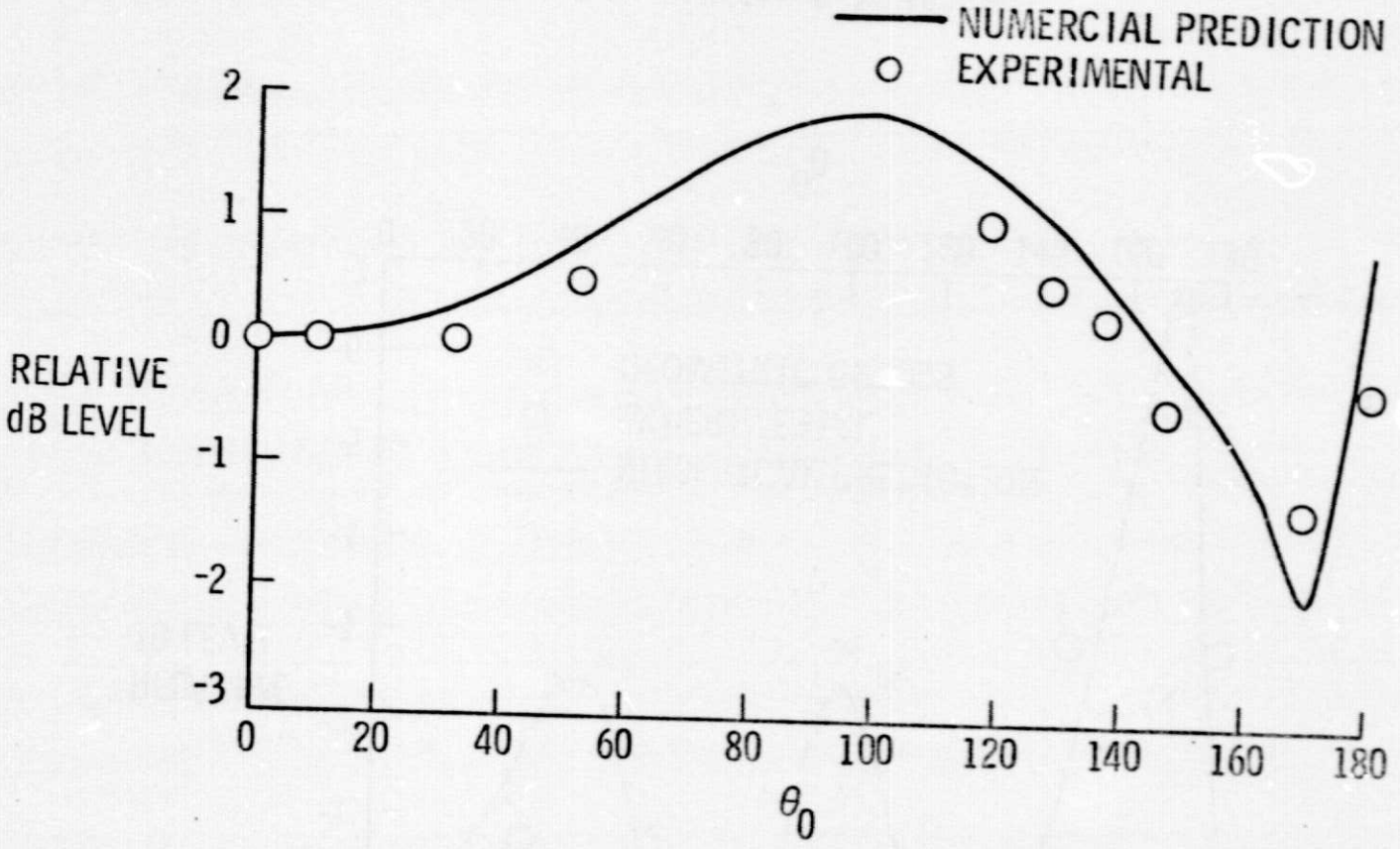

Figure 5. - Relative level decibels for f = 4.11 kHz.

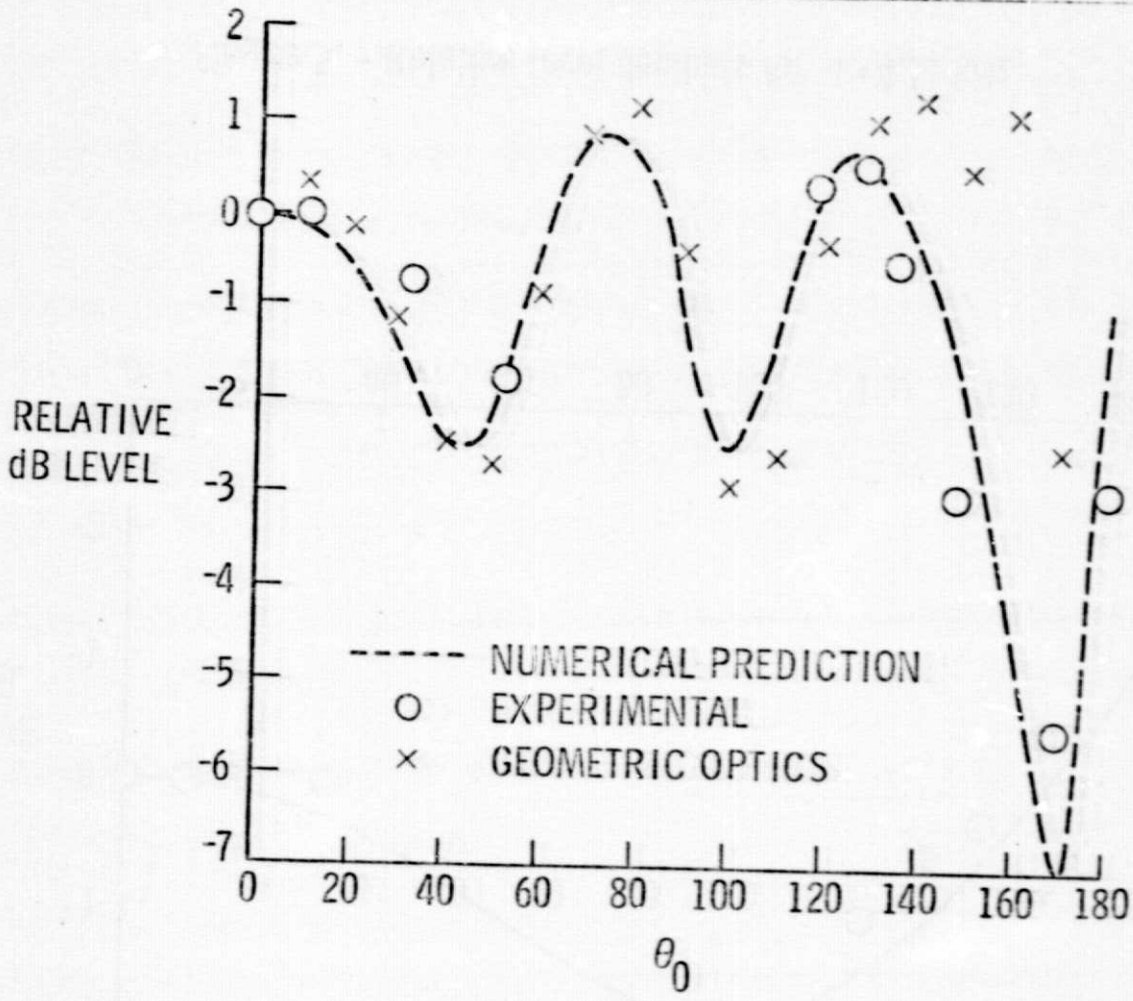

Figure 6. - Relative level decibels for f = 16.44 kHz.

1. Report No.	2. Government Accession No.	3. Recipient's Catalog No.
NASA TM 74098		

4. Title and Subtitle	5. Report Date
Measurements and Analysis of Far-Field Scattering from a Prolate Spheroid	October 1977
	6. Performing Organization Code 2620
7. Author(s)	8. Performing Organization Report No.
A. Bayliss and L. Maestrello	
	10. Work Unit No. 505-03-13-11
9. Performing Organization Name and Address	11. Contract or Grant No.
NASA Langley Research Center Hampton, Virginia 23665	
	13. Type of Report and Period Covered Technical Memorandum
12. Sponsoring Agency Name and Address	14. Sponsoring Agency Code
National Aeronautics and Space Administration Washington, DC 20546	

15. Supplementary Notes
Paper presented at the Acoustical Society of America Meeting, Miami Beach, Florida, December 13-16, 1977.

16. Abstract
The far-field acoustic scattering by a prolate spheroid with axial point sources near the tip of the body was measured. Data were taken for ka between 10-160 where (a) is the semi-major axis of the spheroidal. Comparisons were made with numerical results obtained by an integral equation based on the simple source method with appropriate coordinate stretching introduced to permit high frequency solutions with a minimal number of grid points. Theory and experiment agree within experimental error except for the highest frequencies in the shadow region, where very rapid changes in pressure make precise measurements difficult. The results show that for frequencies of aeroacoustic interest, the scattered field is very large and cannot be ignored.

17. Key Words (Suggested by Author(s))	18. Distribution Statement
Acoustic Scattering 71 Jet Noise	Unclassified Unlimited

19. Security Classif. (of this report)	20. Security Classif. (of this page)	21. No. of Pages	22. Price*
Unclassified	Unclassified	20	$3.50

* For sale by the National Technical Information Service, Springfield, Virginia 22161